PNAS RESEARCH ARTICLE | NEUROSCIENCE

Multilevel atlas comparisons reveal divergent evolution of the primate brain

Clément M. Garin[a,1], Marie Garin[b], Leonardo Silenzi[c], Rye Jaffe[a,c], and Christos Constantinidis[a,d,e,1]

Edited by Ranulfo Romo, Universidad Nacional Autonoma de Mexico, Mexico City, D.F., Mexico; received February 12, 2022; accepted April 25, 2022

Whether the size of the prefrontal cortex (PFC) in humans is disproportionate when compared to other species is a persistent debate in evolutionary neuroscience. This question has left the study of over/under-expansion in other structures relatively unexplored. We therefore sought to address this gap by adapting anatomical areas from the digital atlases of 18 mammalian species, to create a common interspecies classification. Our approach used data-driven analysis based on phylogenetic generalized least squares to evaluate anatomical expansion covering the whole brain. Our main finding suggests a divergence in primate evolution, orienting the stereotypical mammalian cerebral proportion toward a frontal and parietal lobe expansion in catarrhini (primate parvorder comprising old world monkeys, apes, and humans). Cerebral lobe volumes slopes plotted for catarrhini species were ranked as parietal∼frontal > temporal > occipital, contrasting with the ranking of other mammalian species (occipital > temporal > frontal∼parietal). Frontal and parietal slopes were statistically different in catarrhini when compared to other species through bootstrap analysis. Within the catarrhini's frontal lobe, the prefrontal cortex was the principal driver of frontal expansion. Across all species, expansion of the frontal lobe appeared to be systematically linked to the parietal lobe. Our findings suggest that the human frontal and parietal lobes are not disproportionately enlarged when compared to other catarrhini. Nevertheless, humans remain unique in carrying the most relatively enlarged frontal and parietal lobes in an infraorder exhibiting a disproportionate expansion of these areas.

evolution | cortex | prefrontal | frontal | parietal

Significance

The evolution of the primate brain has been a matter of debate. Although prior studies have claimed expansion in the frontal lobe of humans, more recent studies have challenged this assertion. We therefore devised an objective methodology to evaluate the relative expansion of different brain areas based on available digital atlases that we called prediction interval deviation matrices. We ultimately found disproportionally greater expansion in the frontal and parietal lobes of catarrhini when compared to other mammalian species. Our results provide evidence that the brain of catarrhini prioritized the development of regions related to higher cognitive functions over auditory or visual areas.

The evolution of the brain is commonly framed within the context of "concerted" versus "mosaic evolution" (1). These theories propose that brain architecture is shaped by either scaling laws that force specific regions to grow concomitantly (concerted) (2), or/and by "rare" shifts in natural selection that lead to unexpected or unscaled size of particular region(s) (mosaic evolution) (3). However, there is still debate in regard to their relative influence on the modification of brain anatomy.

The prefrontal cortex (PFC) accounts for 30% of the human brain's total cortical area (4) and plays a central role in high-order functions, including cognitive control, impulse inhibition, working memory, emotional processes, decision-making, imagination, and language (4, 5). Several PFC regions were reported to have emerged during early primate and anthropoid evolution (6, 7). While conventional wisdom would point toward mosaic evolution to explain the disproportionately larger PFC in humans compared to nonhuman primates (5, 8), Barton et al. (9) raised the possibility that this assumption may be wrong. Additional findings have also lent empirical support to the idea that allometric scaling accounts for neocortex evolution, consistent with the idea of concerted evolution (2, 10). Shedding new light on this controversial topic is therefore essential for settling this debate.

Donahue et al. (8) found that human PFC gray matter volume was 1.9-fold and 1.2-fold greater when compared to macaques and chimpanzees, respectively. These results would seem to demonstrate that the human PFC occupies a larger proportion of the cerebral cortex than the PFC of chimpanzees or macaques. However, Donahue's method was criticized as "an un-scaled measure that does not take into account the fact that some brain structures change at different rates as brain and body sizes grow" (11). Moreover, cortical expansion does not necessarily equate to an increase in functional ability; biological structures with different proportional volumes across species may ultimately serve equivalent functionalities based on a variety of other factors, including structural context, resources consumed, and more (12).

The nearly exclusive focus of current literature on the primate PFC has resulted in a limited perspective (8, 9). Primates display phylogenetic and anatomic similarities, which facilitates comparisons across species, but also shortens the time window in which anatomical modulations may be observed via ecological pressure. Expanding our

Author affiliations: [a]Department of Biomedical Engineering, Vanderbilt University, Nashville, TN 37235; [b]Département de Mathématiques, Université Paris-Saclay, ENS Paris-Saclay, CNRS, Centre Borelli, Gif-sur-Yvette, F-91190 France; [c]Department of Neurobiology and Anatomy, Wake Forest School of Medicine, Winston Salem, NC 27157; [d]Program in Neuroscience, Vanderbilt University, Nashville, TN 37235; and [e]Department of Ophthalmology and Visual Sciences, Vanderbilt University Medical Center, Nashville, TN 37232

Author contributions: C.M.G. designed research; C.M.G. and M.G. performed research; C.M.G., M.G., and L.S. analyzed data; C.M.G., M.G., R.J., and C.C. wrote the paper; and C.C. provided feedback on analysis.

The authors declare no competing interest.

This article is a PNAS Direct Submission.

[1]To whom correspondence may be addressed. Email: clement.garin@vanderbilt.edu or Christos.Constantinidis.1@vanderbilt.edu.

This article contains supporting information online at http://www.pnas.org/lookup/suppl/doi:10.1073/pnas.2202491119/-/DCSupplemental.

Published June 14, 2022.

perspective beyond primate species may thus contextualize the evolution of the primate/human brain. This idea is supported by a larger relative frontal lobe in primates compared to carnivore species (13). We therefore aimed to address the key question of identifying which anatomical brain regions/lobes were disproportionally expanded in humans and other primate species when compared to other mammals.

Our approach lay in using homologous segmentation of brain areas to compare brain volumes across mammalian species. This presented a challenge, as traditional histological volume quantification in the whole brain is currently impractical. However, three-dimensional (3D) atlases of various species (humans, macaques, mouse lemurs, mice, etc.) have been recently published to digitally reveal histological and functional boundaries (14–17). The segmentations of these atlases were often based on cytoarchitecture, as well as a variety of magnetic resonance imaging (MRI) techniques, including functional MRI, diffusion tensor imaging, and MRI contrast (18–20). We identified 20 3D digital brain atlases of 18 mammalian species and adapted each of them into a common anatomical classification to cover the whole brain. We then compared all possible combinations of region volume pairs with prediction interval deviation matrices (PIDMs), a method that we developed in order to analyze large datasets based on phylogenetic generalized least squares (PGLS). We ultimately revealed that the frontal and parietal lobes were both disproportionately expanded in catarrhini compared to other mammalian species.

Results

Developing a Method of Comparison across Atlases. Our analysis used 20 brain atlases from 18 mammalian species, that were published between the years 2013 and 2021 (*SI Appendix*, Table 1). Each of these atlases possesses a different nomenclature with a different granulometry, so a common terminology was required to permit interspecies comparisons. This issue was further complicated by the different levels of segmentation that were utilized across the original atlases (e.g., cortex > frontal lobe > PFC > Brodmann area [BA] 9). However, we overcame the problem by classifying four segmentation levels that could encompass most of the original granulometry (*SI Appendix*, Table 2). This interspecies categorization was founded on other atlases using an incremental segmentation [mice (21), marmosets (22), macaques (14), and humans (23)] and can be depicted as the following:

1. **Level 1** is composed of the neocortex, the cortical white matter, the cerebellum and the brainstem.
2. **Level 2** is composed of the subcortical structures and a subdivision of the neocortex that is composed from a collection of different lobes:
   a. The posterior limit of the frontal lobe was defined as being anterior to the central sulcus (thus separating the motor and somatosensory cortex) in primates. The limits of the frontal cortex were defined caudally by the sylvian and genual sulcus in dogs (24) or by the dorsal part of the motor cortex in cats (25), due to the central sulcus being absent in carnivores. The original ferret atlas did not provide a clear definition of lobar boundaries, leading to its exclusion in any analyses on level two and higher. The posterior limit in sheep was defined by the ansate sulcus, as demonstrated by the 2017 study of John et al. (26), with the sole exception of the somatosensory region, which was reassigned to the parietal lobe. The boundaries between the motor and somatosensory cortices in rodents and pigs were defined as the posterior limit of the frontal lobe.
   b. The limits of the temporal lobe were defined directly beneath the lateral fissure in primates and by the sylvian, ectosylvian, and posterior composite gyri in dogs (24). These limits were already provided in the original segmentation for cats and pigs, and were defined by the suprasylvian sulcus in sheep (26). The limits of the temporal lobe in rodents were supported by the hierarchical segmentation of the Allen brain atlas (21). Notably, in all species, the hippocampus was considered a separate entity (i.e., the hippocampus is not included in either cortical lobes or subcortical areas, since no consensus has yet been established in the literature).
   c. The parietal lobe lies caudal to the motor cortex for all species, encompassing both somatosensory regions, and the parietal association cortex. In dogs, the splenial and suprasylvian fissures defined the medial and lateral borders, respectively (24). In sheep, the ectolateral and suprasylvian gyri defined the borders of the temporal lobe (26).
   d. Occipital parcellation was defined caudally to the parietal lobe and involved various visual areas such as the V1 cortex (BA 17), as well as the extrastriate cortex.
3. **Level 3** is composed of functionally related cortical regions:
   a. The frontal lobe was divided into the orbital frontal cortex (gustatory cortex, orbital proisocortex and preiallocortex), the medial PFC (BA 32, 14, 24, 25), the dorsolateral PFC (BA 10, 9, 46, 8, 55, 33, 9/46) and the ventrolateral PFC (BA 47, 45, 44, the precentral opercular area, and the inferior frontal sulcus). The PFC and the cingulate were added as intermediate level 3 of segmentation. The primate PFC was defined as a combination of the medial PFC, the dorsolateral PFC, and the ventrolateral PFC. The rodent PFC was defined as a combination of the orbital frontal regions, the prelimbic areas, the secondary motor cortex, and area 24 (27, 28). In pigs and cats, the PFC was already defined in the original version of the atlas. The sheep PFC was defined as the anterior cingulate cortex and the orbital gyrus (gyrus proreus) (29). Finally, the canine PFC was defined as a combination of area pregenualis, area genualis (anterior cingulate), area prorealis, area subgenualis, area precruciata medialis, and area subprorealis (30, 31). In all species, the cingulate cortex was a combination of the medial PFC and the medial parietal cortex (see level 3c).
   b. The temporal lobe was divided in three subareas: the auditory regions (BA 41/42, belt, parabelt), the ventral lateral regions (ectosylvian area, the superior temporal sulcus, the fundus of medial superior temporal [FST], the temporal association area, BA 22, BA 21, BA 20, BA 38), the inferior temporal regions (BA 35/36 [perihinal, ectorhinal cortex] and BA 28 [entorhinal]).
   c. The parietal lobe was divided into somatosensory areas, the posterior parietal cortex (parietal association cortex such as BA 5, 7, 40, 39), and the posterior medial cortex (PMC; BA 23, 31 and the retrosplenial cortex).
   d. Subcortical regions were divided into the striatum, pallidum, hypothalamus, and thalamus.
4. **Level 4** is composed of BA segmentation.

We created a table with the correspondence between the original labels of the atlases and our labels according to the segmentation rules in *SI Appendix*, Table 2. This table was employed to

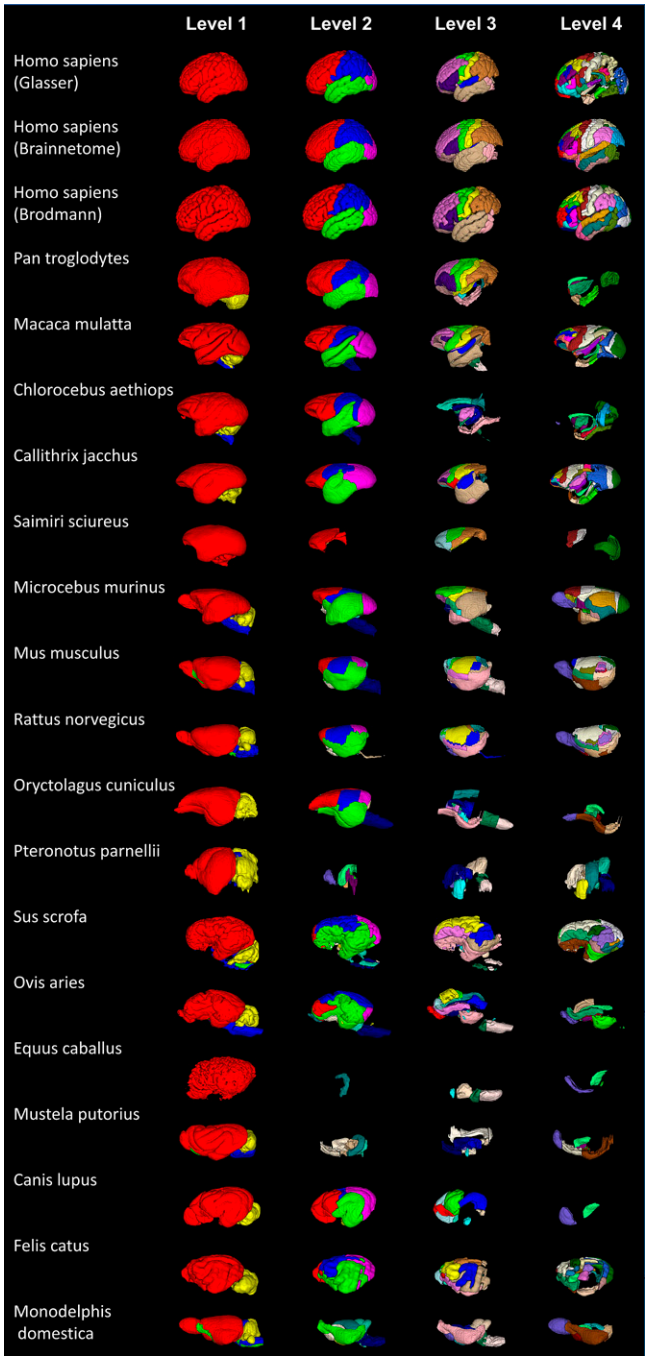

Fig. 1. Mammalian atlases resegmentation at four levels. Twenty atlases from 18 species were organized across four levels of segmentation. Level one corresponds to the neocortex (red), cerebral white matter (green), cerebellum (yellow), and brainstem (blue). Level two corresponds to a division of the cortical lobes, as well as subcortical structures. Level three primarily groups adjacent regions with analogous functions (motor, somatosensory, etc.). Level four is based primarily on Brodmann area segmentation.

reattribute the original regions to new labels (Dataset S1), resulting in four new atlases for each of the 18 species (including three human atlases) (Fig. 1).

Relative Expansion of the Cerebral Lobes: Catarrhini vs. Other Mammals. We used Analysis of Functional NeuroImages (AFNI) (32) to extract the volume of each brain region, and then performed PGLS analysis through the R-language library caper (33). Previous literature has established a need to account for any methods of statistical analysis that factor in phylogenetic relationships through species nonindependency (34). Indeed, species sharing common ancestry are assumed to have more similar residuals from the least squares analysis. We thus used PGLS to statistically compare brain volumes across species. PGLS is a generalized least squares regression that uses phylogenetic relationships to estimate expected covariance in cross-species data (35). This choice of method entails the selection of an area as a regressor. The regressors selected by most previous studies were the nonfrontal neocortex, the white matter, the visual areas, or the insula volume (8, 9, 34).

As a first step, we featured PGLS analyses by plotting the lobar volumes of both catarrhini (vervet, macaques, chimpanzees, and humans) and noncatarrhini mammalian species (Fig. 2). We used the lobe displaying the lowest slope as scale (occipital in catarrhini; Fig. 2*A*, parietal in other mammals; Fig. 2*B*). We measured the slope in catarrhini (where a linear relationship could be observed, Fig. 2, red) and in the noncatarrhini mammalian group (Fig. 2, black). A bootstrap procedure (see *Materials and Methods*) was then performed to provide statistical support for the separation of these two groups of species. To do so, we evaluated the random distribution of the slope differences that we obtained by arbitrarily assigning species to two distinct groups. Then, we derived the 95% empirical bootstrap confidence interval of the slope differences for the six plots presented in Fig. 2 *A* and *B* (*SI Appendix*, Table 3). We found that the difference of slopes between catarrhini and other mammals always fell outside the confidence interval for all comparisons except for frontal vs. parietal (as expected) (*SI Appendix*, Table 3). These results indicate with high probability that the differences observed between the slopes of the two groups were not due to chance. We may therefore conclude that the lobar slope of catarrhini species is significantly different from other noncatarrhini mammalian species.

Our next step was proposing a classification of lobar expansion based on their slopes (Fig. 2). In catarrhini (red curve), the slope of the parietal (slope = 1.44; 1.22:1.63), frontal (slope = 1.32; 1.02:1.63), and temporal (slope = 1.23; 0.959:1.63) cortices displayed a hypermetric (slope >1) tendency when compared to the occipital lobe (Fig. 2*A*, red). We found that the parietal lobe displayed the highest slope, while the temporal and occipital lobes displayed the second lowest and lowest slopes, respectively.

We performed a sensitivity analysis with respect to the human atlases i.e., we repeated these analyses using three different human atlases that are heretofore referred to as the Glasser (36), Brainnetome (23) and Brodmann (18) atlases, in order to evaluate any segmentation dependencies (*SI Appendix*, Figs. 2 and 3). The resulting slopes could be classified in a similar order, with the exception of the frontal and parietal lobes (with Brodmann segmentation frontal slope = 1.61 and parietal slope = 1.58 [*SI Appendix*, Fig. 3]). In other mammalian species (Fig. 2*B*, black curve), the same classification scaled by the parietal lobe (the lobe displaying the lowest slope) gave us the following results: occipital (slope = 1.12; 0.679:1.55), temporal (slope = 1.06; 0.922:1.2), and frontal (slope = 1.01; 0.718:1.3).

We then performed PGLS analysis to determine if the volume of the catarrhini frontal and parietal lobes deviate from the prediction interval. This was carried out by defining the sample (noncatarrhini mammals; open symbols in Fig. 2) on which the prediction intervals could be calculated and excluding the group of species of interest (catarrhini; Fig. 2; red filled symbols). Although we found that human and chimpanzee frontal lobes lie beyond the prediction interval, macaque and

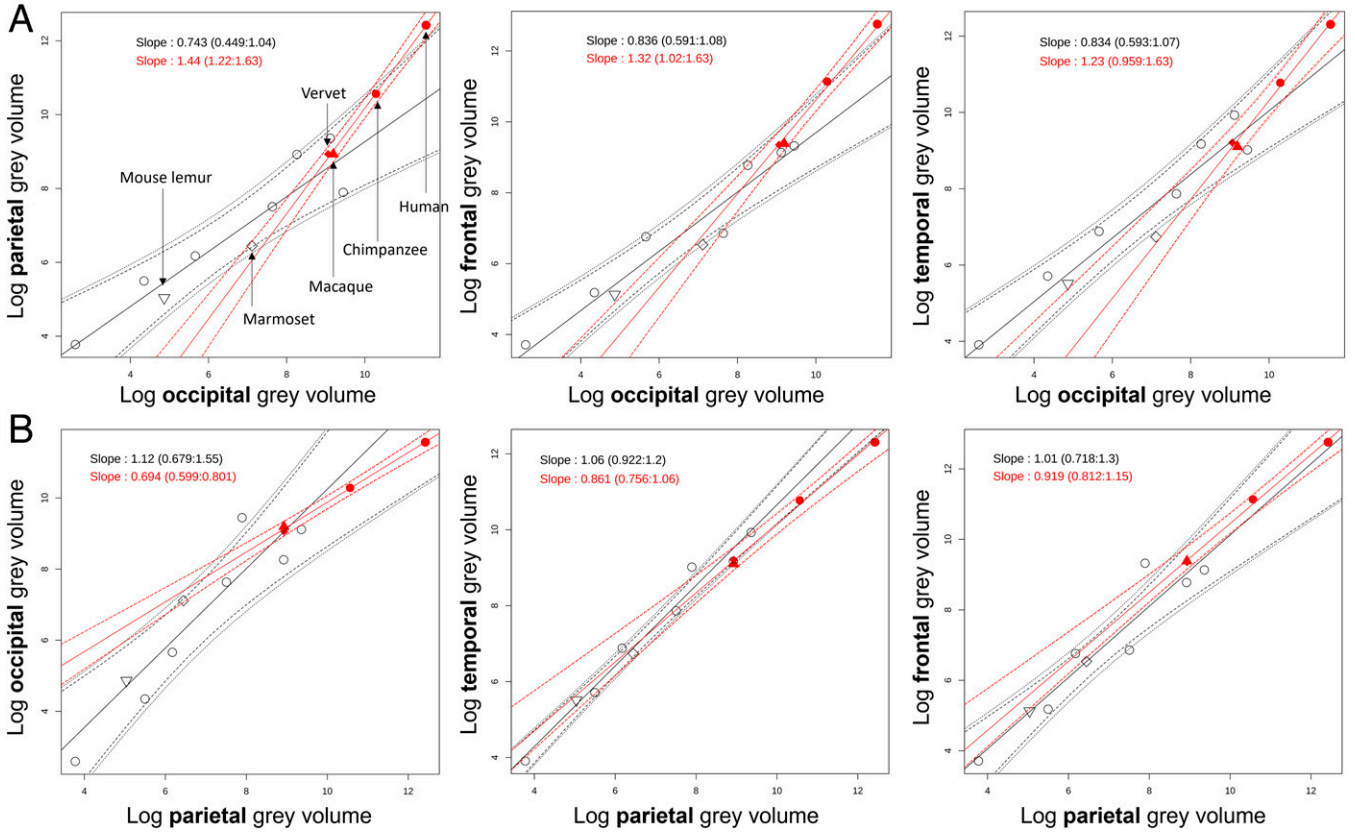

Fig. 2. PGLS analyses based on the volumes of the four mammalian cerebral lobes. The red regression lines, prediction intervals, and confidence intervals were calculated for catarrhini (vervets, macaques, chimpanzees, and humans -red filled symbols). Likewise, the black regression lines, prediction intervals, and confidence intervals were calculated for noncatarrhini mammals (open symbols). PGLS analyses were scaled by the regions possessing the lowest slope and classified separately based on slope value of catarrhini (*A*, red curve), and noncatarrhini mammals (*B*, black curve). Slope values and confidence intervals are indicated on the plot. The human atlas by Glasser was used for this analysis.

vervet frontal lobes do not. Moreover, we also found that the frontal and parietal lobes of other primate species, such as marmosets and mouse lemurs, were below the regression line. We evaluated segmentation dependencies by repeating each analysis for the three different human atlases (18, 23, 36) (*SI Appendix*, Figs. 2 and 3). We found that the human frontal lobe was always beyond the prediction interval, regardless of which atlas was used for comparison. Moreover, humans were the only species for which the parietal lobe also lay beyond the prediction limit. By contrast, the temporal lobes of all catarrhini were found within the prediction limits when compared to the occipital lobes. Although using the least expanded lobe as regressor for PGLS analysis could lead to an overestimation of the frontal and parietal lobe expansion, we sought to overcome this limitation by applying a wide range of regressors to test if each primate species (humans, chimpanzees, macaques, vervets, marmosets, and mouse lemurs) carried individual characteristics of expansion in any regions.

Prediction Interval Deviation Matrices: A Method for Capturing Volumetric Expansion across the Whole Brain. Whole brain comparisons between each pair of homologous regions can be summarized in matrix form (Figs. 3–5). We developed a method that we refer to as prediction interval deviation matrices. This method allowed us to hierarchically organize the PGLS results (prediction interval deviation) and to test every possible combination of variables. These matrices were produced for humans (Fig. 3 and *SI Appendix*, Fig. 4), chimpanzees, macaques (Fig. 4), vervets (*SI Appendix*, Fig. 4), marmosets, and mouse lemurs (Fig. 5). Prediction interval deviation matrices (PIDMs) were obtained by performing PGLS analyses across all possible combinations of region pairs.

Globally, PIDMs evaluate if the volume of all available regions in a given atlas (rows) fell outside (red or blue squares) the 95% prediction interval when compared to the same list of regions used as scale (columns). Variables of each PIDM include any regions of any level extracted from each atlas, as well as body and brain mass. The differences between the actual value and the prediction interval were reported (scale bar) for all regions falling outside this interval. The comparisons leading to an optimization error for the computation of Pagel's λ (a parameter that permits the attenuation of weight allocated to phylogeny) or with less than five species (after removing the species of interest) are represented by gray squares in the PIDM. Each matrix was ordered based on the number of values falling outside the prediction interval. If two regions possessed the same number of significant deviations, the average of their matrix rows (that is, the distance between the data point and the prediction interval of each comparison when this point was located beyond the interval) would be calculated for ranking.

In humans, the Glasser atlas (37) (Fig. 3*A*) revealed the retrosplenial, frontal, parietal areas, PFC, and cingulate areas to be the five regions (red) with the lowest conformity to allometric relationships, with a higher volume than expected when compared to other species. By contrast, the body mass, BA 17, auditory regions, brain mass, and white matter all fell below the prediction interval when compared to enlarged regions.

The Brainnetome atlas (23) (Fig. 3*B*) revealed the parietal, frontal, neocortical, and prefrontal areas, as well as BA 4, to be among the regions with the lowest conformity to allometric

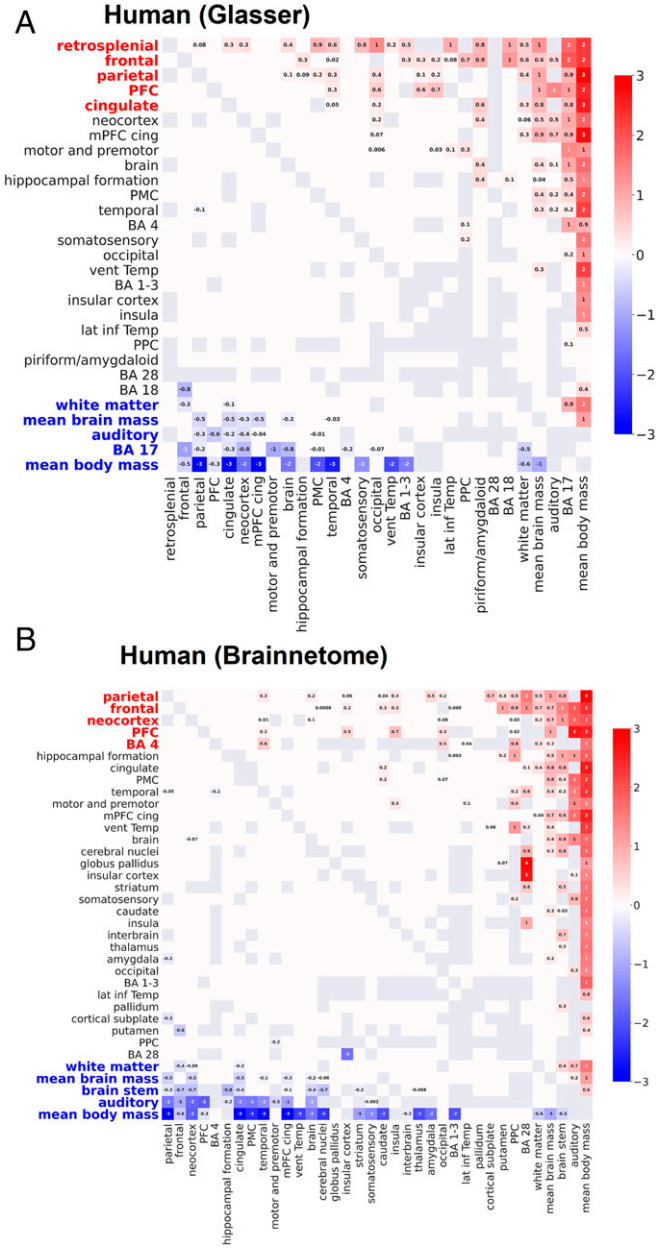

Fig. 3. Prediction interval deviation matrices based on the human atlases of Glasser (*A*) and Brainnetome (*B*). Matrix recapitulating the results of PGLS analyses performed between all pairs of regions. A pair of regions was included if there were at least five species for which corresponding volumes were available. Region pairs that were not included are represented in gray squares. For each pair, we evaluated if the volume of a human region (rows) falls outside the 95% prediction limits when scaled by the region in columns. Regions falling outside the 95% prediction limits were included in the colormap. Otherwise, their value was set to zero. The matrix was ordered based on the number of values falling outside the prediction interval. Frontal, prefrontal, and parietal cortices were classified in the top five (red) expanded regions in both atlases. Furthermore, the majority of brain regions were found to be expanded when compared to body mass. Color scale: distance between the data point value and the projection on the prediction interval when falling outside of it (in logarithmic units).

relationships. Body mass, auditory regions, brainstem, brain mass, and white matter fell consistently below the prediction interval when compared to enlarged regions. The retrosplenial area was not visible in this matrix, as this was not segmented in the original classification. Subcortical regions such as the globus pallidus, putamen, and striatum, as well as some cortical regions such as the amygdala, BA 1–3 or the somatosensory cortex, were generally on the regression line. The Brainnetome was the only human atlas to examine subcortical regions.

Finally, the Brodmann atlas (*SI Appendix*, Fig. 4) (18) revealed the frontal lobe, PFC, total brain volume (brain), motor and premotor, and parietal areas to be among the regions with the lowest conformity to allometric relationships, with a higher volume than expected when compared to other species. By contrast, mean body mass, auditory regions, BA 17, insula, and PPC all fell below the prediction interval when compared to enlarged regions.

Human regions with least recurrent conformity to the allometric relationships (PFC, retrosplenial, and auditory cortex) are plotted in *SI Appendix*, Figs. 5–7, revealing differences in deviation from the allometric prediction when these regions are scaled by the occipital or the parietal lobe. For example, the

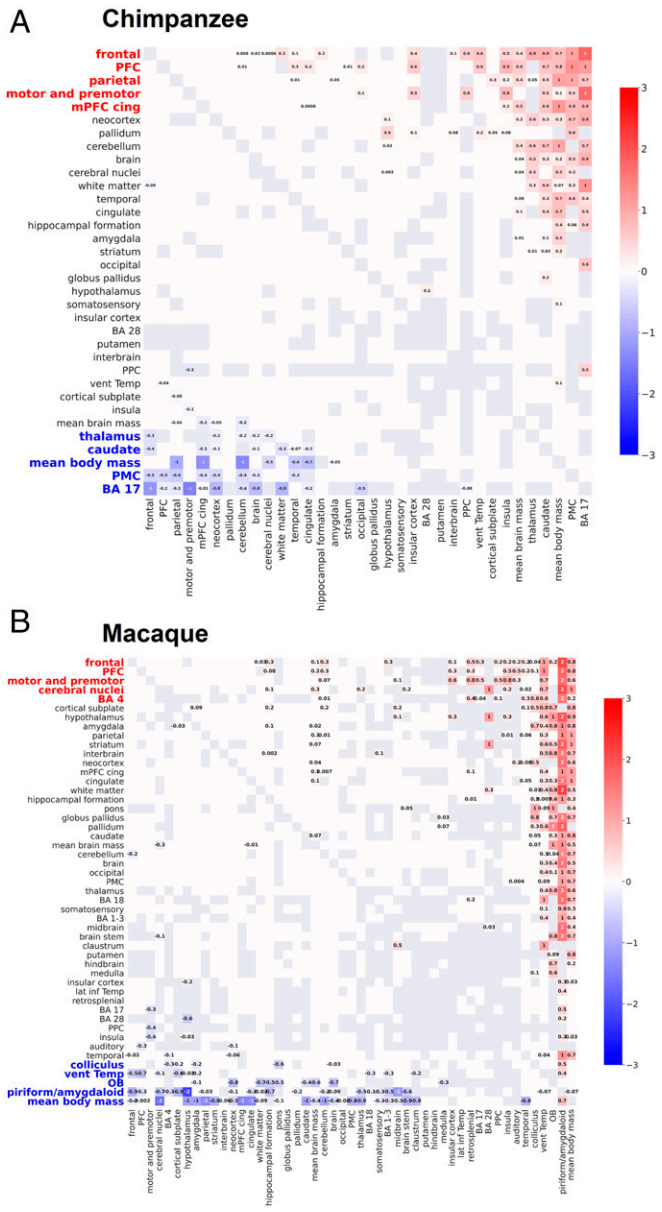

Fig. 4. Prediction interval deviation matrices based on the chimpanzee (*A*) and macaque (*B*) atlases. As with humans, the frontal and prefrontal cortices were classified in the top five (red) expanded regions in both species. Once again, most brain regions were found to be expanded when compared to body mass. Moreover, the chimpanzee parietal and BA 17 were also classified in the top five most and least expanded regions, respectively. However, this did not apply to macaques.

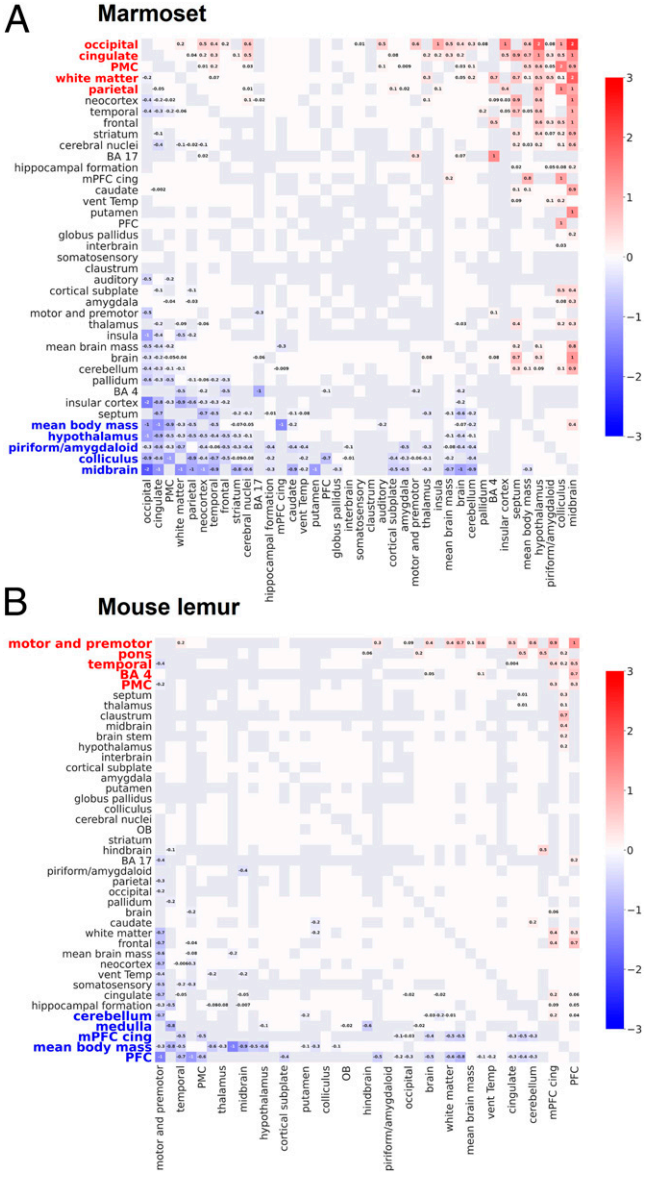

Fig. 5. Prediction interval deviation matrices based on the marmoset (*A*) and mouse lemur (*B*) atlases. Noncatarrhini primates contrasted catarrhini primates, as the frontal regions were not classified in the top five (red) most expanded regions. The marmoset occipital and frontal lobes were found to be the most and least expanded, respectively. The mouse lemur temporal and frontal lobes were found to be the most and least expanded, respectively.

volumes of auditory regions displayed an isometric trend, with humans beings below the prediction interval only when compared to parietal regions (*SI Appendix*, Fig. 3*C*).

This pattern of expansion was not universal across all primates, but similarities are observed across catarrhini species. The most expanded areas identified were the frontal, prefrontal, parietal, motor and premotor, mPFC/cingulate in chimpanzees (Fig. 4*A*); the frontal, prefrontal, motor and premotor, cerebral nuclei, and BA 4 in macaques (Fig. 4*B*); the frontal, white matter, neocortical, parietal areas, and the cerebral nuclei in vervets (PFC was not included in this segmentation; *SI Appendix*, Fig. 4); the occipital, cingulate, PMC, white matter, and parietal in marmosets (Fig. 5*A*); and the motor and premotor, pons, temporal, BA 4, and PMC in mouse lemurs (Fig. 5*B*). By contrast, the least expanded areas identified were BA 17, PMC, body mass, caudate, and the thalamus in chimpanzees (Fig. 4*A*); the body mass, piriform/amygdaloid, olfactory bulbs, ventral temporal, and colliculus in macaques (Fig. 4*B*); the olfactory bulbs, body mass, PMC, septum and amygdala in vervets (*SI Appendix*, Fig. 4); the midbrain, colliculus, piriform/amygdaloid, hypothalamus, and body mass in marmosets (Fig. 5*A*); and the PFC, body mass, mPFC/cingulate, medulla, and cerebellum in mouse lemurs (Fig. 5*B*).

The PIDMs globally reveal expansion across most cerebral regions when compared to body mass in primates. BA 17 was found among the five regions with the most negative deviation from the regression line in humans and chimpanzees, thus suggesting a relatively lower increase in the primary visual volumes of apes. PIDMs simultaneously classified the frontal lobe, the PFC, and the parietal lobe as being among the five regions with the greatest deviation from the allometry in macaques, chimpanzees, and humans. Notably, the occipital lobe appeared to be the most expanded area in marmosets, thus contrasting with the catarrhini's classification. Furthermore, the frontal lobe's absence in the top five expanded regions was confirmed in mouse lemurs, with the temporal lobe being the most expanded instead. The slope, intercept, and estimated Pagel's λ value for the relationship between each pair of regions for each species are presented in *SI Appendix*, Figs. 8–15.

Discussion

In this study, we identified anatomical regions with disproportionate expansion in the primate brain by conducting a large-scale interspecies comparison. We reorganized all brain regions into four common levels of segmentation to generate an interspecies categorization that would be flexible to the granulometry of different atlases. We were thus able to measure the volume and slope of different regions/lobes across the whole brain of various mammalian species at different levels of segmentation. We found that the evolution of catarrhini may have prioritized the expansion of frontal and parietal lobes, while the evolution of noncatarrhini mammals may have prioritized the expansion of the occipital and temporal lobes instead. PIDMs allowed confirmation for the results obtained using the slope classification of the cerebral lobes (Fig. 2). PIDMs further indicated the PFC as the most significant driver of the disproportionate expansion that was observed in the catarrhini frontal lobe. An emergence of PFC areas with reduced myelination and homotypical architecture was found specifically in anthropoid species (6, 7). The emergence of these regions, rather than the expansion of preexisting areas, may serve as a possible mechanistic explanation for the "mosaic evolution" behavior of the catarrhini PFC. It is important to note that in several primate species, motor and premotor areas and/or BA 4 seem also to be involved in the frontal expansion but at a lower level than PFC.

The regions responsible for the disproportionate expansion of the parietal lobe were more difficult to investigate, due to the absence of homology across species for most of the parietal areas. However, the somatosensory cortex was not found among the top five most expanded regions in the parietal lobe, thus implying a greater likelihood of other areas being responsible. In particular, the retrosplenial cortex presents a possible candidate to explain the expansion of the parietal cortex in humans. Future research may also investigate the relatively lower volume/mass for the human occipital lobe, auditory regions, BA 17, and the relationship of brain volume to body mass.

The pattern of expanded regions (frontal, parietal, PFC, and BA 4) in catarrhini partially fit with the expanded regions found when macaque brain areas were registered to a human atlas (38). These results reveal a disproportionate expansion of the prefrontal, parietal, and temporal association areas in the

neocortex. Van Essen et al. (37) hypothesized that myelinated brain areas (such as lower, unimodal cortices, including the primary visual, auditory, motor, and somatosensory cortices), correspond to areas with reduced expansion. This assumption was partially verified, except for motor and premotor areas, which were also found to be expanded (though more modestly than prefrontal areas). Thus, this result suggests that disproportionate expansion is not exclusive to lightly myelinated areas. The primate motor system was shown to receive input from the PFC (39), to be refined in primates (especially in catarrhini, e.g., regarding the control of fingers), and to be associated with development of high order cognitive functions (40). Several overexpanded human brain regions were also identified in the human default mode network, thus supporting the expansion of DMN components over the course of hominoid evolution (41). The strengthening of long-distance connections, such as PMC-mPFC, may also be reflected as a volume gain of these regions in humans.

Advantage of PIDM and Atlas-Based Approach. Most brain atlases used in our study were generated based on mean MRI anatomical images to limit the interindividual variability impact. PGLS analyses allowed volumetric prediction interval deviations to be computed across primate species without any a priori assumptions of the over/underdeveloped regions, thus decreasing dependencies on any region used as a regressor. We developed PIDMs for volumetric comparisons between each pair of possible regions across all of the examined atlases. The use of this technique combined with our volumetric measures overcame a variety of limitations from previous studies, including the processing of histological sections, which causes distortions/shrinkage and undermines volumetric measures (17). Prior PGLS analyses did not picture the whole brain and were thus limited to scaling their measurements across only one or two anatomical regions (8, 9, 34). Our method, however, allowed a large number of regions/regressor couples to be examined. In addition, few prior studies included nonprimate mammalian species, resulting in a limited evolutionary perspective. PIDMs revealed a comprehensive picture of the relative regional expansion of the brain in a given species and thus, we discourage the future use of nonfrontal neocortex as scale for PGLS analysis, due to this area possessing multiple expanded regions.

A Scale to Predict the Evolution of the Brain. PIDMs highlight the importance of the chosen regressor when computing intervals of expected brain volumes through PGLS analysis. Indeed, most of our examined brain regions were significantly out of the prediction interval when comparing under and overexpanded regions (the two extremes of the PIDM). PIDMs reveal that the majority of the regions scaled by body mass in primate species are consistently found enlarged. This result implies that primates possess expanded brain volume when compared to nonprimate species and is consistent with the outcomes of previous studies showing that when allometry is accounted for, primates generally have relatively large brains compared to other mammals (42). PIDM analysis further demonstrated that not all regions/lobes grow uniformly, with specific regions acting as the primary drivers of primate encephalization (mosaic evolution).

PIDMs also corroborate our bootstrap results and allowed us to propose that the relative overexpansion of frontal areas may be observed primarily in catarrhini (this region was not found as expended in marmosets and mouse lemurs PIDM). The proximity of catarrhini cerebral evolution thus explains why the human frontal and prefrontal cortices were not located out of the allometric prediction when compared to other catarrhini species in this study or to other primate species in other studies (9, 43). These findings support the hypothesis that any given species is more likely to exhibit gradual change driven by phylogenetic proximity, rather than an abrupt change at random. Comparing the numbers of PFC neurons in human versus nonhuman primates also demonstrates that evolution occurred along the same allometric trajectory (43), thus emphasizing Barton et al.'s expected human frontal volumes (9, 43). Nevertheless, the human brain is still unique, carrying the most enlarged frontal and prefrontal cortices of an infraorder exhibiting extreme expansion in these areas. Smaers et al. (44) evoked a similar idea by proposing left PFC hyperscaling to be an ape specialization, with the greatest enlargement in humans. Further support is drawn from findings that demonstrate shared relationships between cortical mass and neuronal cell quantity across all primate species, which differs when compared with nonprimates (45). Other supporting evidence demonstrates primate frontal cortex hyperscaling relative to the rest of the neocortex when compared to the carnivorous frontal cortex (13).

Limitations. We advise caution against the overinterpretation of our results. As demonstrated by Georg F. Striedter in his "Principles of Brain Evolution," there is still a heated debate in regard to how the size of a given region, the number of neurons and synapses, or other factors correlates with the modification of behavioral complexity (1). We do not wish to take a position in this so-called "bigger is better" debate, as we did not attempt to directly relate the size of the PFC to specific cognitive abilities. Moreover, without knowing the specific neural substrates (neuronal size, density, architecture, etc.) responsible for the improvement of any given cognitive function, we cannot directly generalize volumetric observations into evolutionary rules. Here, we use volumetric measures to identify (in catarrhini) and localize (in the frontal and parietal cortices) significant evolutionary events that could have played a key role in the development of our species' current cognitive abilities. Biomarkers such as functional MRI, tractography, positron emission tomography, and cognitive test performance will be necessary to further explain if and how "bigger can be better."

Despite the extraordinary amount of information that was extracted from our datasets, several limitations of segmentation and cross-species homologies must be taken into account. First, the accurate delineation of the PFC is still an open debate in the mammalian brain (4, 8, 27). For example, Laubach et al. (27) established that there was little consensus between researchers on the use of PFC anatomical terms in rodents. Furthermore, there is also limited consensus in regard to the classification of numerous other cerebral structures beyond the PFC (46, 47). In consequence, we cannot rule out that this lack of consensus may have generated variability (or noise) in PGLS analyses.

Another limitation was the definition of lobe/region homology across species. Our methods section provides a justification for our interspecies regional boundaries based on extensive literature, but this is not meant to be conclusive. The absence of any consensus in literature does not currently allow the establishment of any clear homology between species (27) and the variability generated by ongoing debates may have a similar effect to the absence of boundary consensus within species. Previous studies faced similar problems in explaining why the use of primates was preferred for determining the optimal consensus on segmentation (8, 43). However, we previously established that the exclusive use of primates may result in other

limitations, such as shortening the time window in which anatomical modulations may be observed via ecological pressure. Thus, despite the stated limitations, our study provides a thorough evaluation of cerebral evolution based on volumetric measures.

Conclusion. Thanks to the development of a phylogenetic comparative method (PIDM), we conclude that the ancestors of the living catarrhini parvorder may have taken a very different path, 35 million years ago (48), regarding the overexpansion of frontal and parietal regions. Catarrhini prioritized the development of several regions related to higher cognitive functions over auditory or visual areas. This study clarified a long running debate concerning the PFC expansion, by highlighting the importance of using multiple variables as regressor, as well as the importance of including nonprimate species for evolutionary studies.

Materials and Methods

Modification of the Original Atlases into a Common Multilevel Segmentation. Original atlases were downloaded using the references provided in *SI Appendix*, Table 1. We wrote a python script that reattributed the original label file provided by the authors of each atlas, thus allowing the reparcellation of each atlas through either renaming or grouping regions together. A single region, in one species (the cingulate in sheep) was resegmented by hand, in order to separate the frontal from parietal lobe. New labels were defined based on *SI Appendix*, Table 2, which provides a common classification for all species, divided across four levels. The interspecies classification was based on the multilevel segmentation provided by various atlas studies including: the Brainnetome atlas (23), the macaque Charm atlas (14), the marmoset atlas of Liu (49), and the Allen segmentation in the mouse (21). Most of the newly labeled regions (the regions homologous across species) stopped at level 2 or 3 in order to prevent the overinterpretation of homologies across species. For example, in some species such as dogs (*Canis lupus*), sheep (*Ovis aries*), and ferrets (*Mustela putorius*), nomenclature was determined by following major gyri and sulci. As a result, very few equivalences were identified up to levels three and four. Other species, such as the mustache bats (*Pteronotus parnellii*), rabbits (*Oryctolagus cuniculus*), short-tailed opossums (*Monodelphis domestica*), and horses (*Monodelphis domestica*), did not segment or partially segment subcortical/cortical areas in the original atlases. These issues were bypassed by reattributing each region exclusively to a meaningful cross-species level, thus allowing us to maximize the information we could extract from the original atlases. However, there is still significant debate in regard to the boundaries between the different lobes in different mammals, thus allowing debate for our proposed resegmentation as well. Therefore, to support the reproducibility our resegmentation, we provide an exhaustive list of all the modifications performed on the original atlases (Dataset S1). Mean body and brain mass were provided by the study of Burger et al. (42). Finally, using "3dhistog" from AFNI (32), we extracted the volume of each brain region for PGLS analysis.

For some species (horse, squirrel monkey), the segmentation between the white matter and the gray matter was not originally provided. We thus used ANTs (50) with the original template provided by the atlas in order to segment the template in three components (white matter, gray matter, and cerebrospinal fluid). Segmentation was corrected manually using ITKsnap (51) when evidently inaccurate. Given the variation of brainstem quantity included in each template/atlas, only the cortical white matter data were included in our study.

PGLS Analysis. The approach of this work is based on the study of allometric relationships, involving a linear ratio on a logarithmic scale. Regressions are performed between the different volumes of different brain areas across different species. Specifically, PGLS is among the most widely used methods of phylogenetic comparative statistics. Species with shared evolutionary histories are known to produce more similar residuals from the least squares regression line, breaking the basic assumption of independence in traditional statistical models (e.g., ordinary least squares). PGLS accounts for this by modifying the expected phylogenetic covariance matrix, which becomes diagonal when assuming independence between its features. Dependence feature modeling consists of adding off-diagonal elements into the matrix, and relies upon the hypothesis that traits evolve according to a Brownian motion. This modeling method thus accounts for interspecific autocorrelation due to phylogeny. Likewise, Pagel's λ attenuates the weight allocated to phylogeny, being defined as the multiplier of the off-diagonal elements of the expected covariance matrix. This parameter is obtained through maximum likelihood estimation. We used the R-language library *caper* (33) to first perform PGLS on the lobar volumes. Species were separated into two groups (catarrhini and noncatarrhini mammalians) to test both slope differences and any deviations from the prediction interval. Prediction intervals was calculated on the sample (noncatarrhini mammalians) while excluding the species of interest (catarrhini). Slopes and intercepts were also estimated using the model described above for all species available for the two variables considered. On Fig. 2, confidence and prediction intervals tended to overlap, making them difficult to distinguish on the figures, due to the high number of individuals from which the average data were drawn.

Bootstrap Analysis. Statistical evidence for the grouping of the catarrhini and noncatarrhini mammals depicted in Fig. 2 was provided by using bootstrap procedure. Bootstrap analysis was achieved on the lobar volumes by randomly assigning species into two groups. First, the differences between the slope of the group of interest and the associated sample were computed (corresponding to the difference between the slope of the red and black regression line; Fig. 2). Then, we tested if this slope difference was larger than what would be predicted by chance. To do so, we evaluated the random distribution of the slope differences that we obtained by arbitrarily assigning species to two distinct groups of sizes 4 and 10. Here, there are 1001 ways to draw 4 items from a sample of 14 species. We extracted the slope of PGLS calculated on 4 species (with Pagel's λ equal to 1) and then subtracted the slope from the 10 remaining species for each of the 1001 combinations. Next, we derived the 95% empirical bootstrap confidence interval in each of the six comparisons (parietal vs. occipital, frontal versus occipital etc.). Finally, we compared if the observed slope differences between the group of interest and its sample fell within the bootstrap confidence interval (based on the 1001 combinations). The result of both this analysis, and as the observed slope differences, is reported in *SI Appendix*, Table 3.

PIDMs. The method developed in this section aimed to use matrices to highlight which regions display relatively and recurrently severe deviations from prediction intervals for each species of interest. PIDMs were created to recapitulate, in a given species, all possible PGLS analyses based on every possible combination of regions. This analysis was crystallized over the production of matrices presented in Figs. 3–5. Notably, PIDMs included all combinations of two variables, only excluding those with less than or equal to five species after the removal of the species of interest (represented by gray squares). For those "valid" pair of regions, we computed PGLS and reported the prediction interval deviation (i.e., the distance between the actual value of the species of interest and the prediction interval) only if the value falls outside (red or blue squares) the prediction interval. Each matrix was ordered based on the number of values falling outside the prediction interval. If two regions possess the same number of values outside the prediction interval, the average of their matrix rows would be calculated for ranking. Gray squares indicated the computations in which Pagel's λ led to an optimization error. Additionally, if a region was a subsection of another region (e.g., frontal vs. neocortex), the smallest region (frontal) was systematically deduced by the largest (neocortex).

Humans, chimpanzees, macaques, and vervets were all removed for the humans, chimpanzees, macaques, and vervets PIDM. These species, in addition to marmosets, were also removed for the marmosets PIDM. Similarly, all these species, in addition to mouse lemurs, were removed for the mouse lemurs PIDM. Confidence and prediction intervals were estimated using the R-language library *evomap* (34). The functions used to estimate these intervals required the sample size of the estimated future points (k). This parameter (k) was estimated based on the number of subjects used to build each species template. k was estimated based on the lowest sample size of the species of interest ($k = 10$ for catarrhini and mouse lemur species). Although, the marmoset template was built with only one subject ($n = 1$), implying that $k = 1$ should apply when computing its PIDM, $k = 10$ was used for all PIDMs for the sake of comparison (Figs. 3–5). Nevertheless, a PIDM with $k = 1$ in marmoset is presented in

SI Appendix, Fig. 13, in order to show that k value did not artificially change the outcome of the results.

Data Availability. The code for PIDM is freely available and open source at GitHub (https://github.com/MarieGarin/PIDM). Previously published atlases and templates were used for this work which are all freely available online (see *SI Appendix*, Table 1).

ACKNOWLEDGMENTS. We thank Jon Kaas and Stefan Everling for valuable comments on a previous version of the manuscript. We also would like to thank all the authors that shared their atlases online. This work was supported by the National Institute of Mental Health of the National Institutes of Health (R01 MH116675 and R01 MH117996) and by a public grant as part of the Investissement d'avenir project (ANR-11-LABX-0056-LMH), LabEx LMH, and the Région Ile-de-France.

1. G. F. Striedter, *Principles of Brain Evolution* (Sinauer Associates, Inc., Sunderland, MA, 2005).
2. B. L. Finlay, R. B. Darlington, Linked regularities in the development and evolution of mammalian brains. *Science* **268**, 1578–1584 (1995).
3. G. F. Striedter, Précis of principles of brain evolution. *Behav. Brain Sci.* **29**, 1–12, discussion 12–36 (2006).
4. M. Carlén, What constitutes the prefrontal cortex? *Science* **358**, 478–482 (2017).
5. C. C. Sherwood, J. B. Smaers, What's the fuss over human frontal lobe evolution? *Trends Cogn. Sci.* **17**, 432–433 (2013).
6. S. P. Wise, "The evolution of the prefrontal cortex in early primates and anthropoids" in *Evolutionary Neuroscience*, J. H. Kaas, Ed. (Academic Press, London, 2020), pp. 669–707.
7. T. M. Preuss, P. S. Goldman-Rakic, Myelo- and cytoarchitecture of the granular frontal cortex and surrounding regions in the strepsirhine primate Galago and the anthropoid primate Macaca. *J. Comp. Neurol.* **310**, 429–474 (1991).
8. C. J. Donahue, M. F. Glasser, T. M. Preuss, J. K. Rilling, D. C. Van Essen, Quantitative assessment of prefrontal cortex in humans relative to nonhuman primates. *Proc. Natl. Acad. Sci. U.S.A.* **115**, E5183–E5192 (2018).
9. R. A. Barton, C. Venditti, Human frontal lobes are not relatively large. *Proc. Natl. Acad. Sci. U.S.A.* **110**, 9001–9006 (2013).
10. C. J. Charvet, B. L. Finlay, Embracing covariation in brain evolution: Large brains, extended development, and flexible primate social systems. *Prog. Brain Res.* **195**, 71–87 (2012).
11. R. A. Barton, S. H. Montgomery, Proportional versus relative size as metrics in human brain evolution. *Proc. Natl. Acad. Sci. U.S.A.* **116**, 3–4 (2019).
12. K. Schmidt-Nielsen, *Scaling* (Cambridge University Press, Cambridge, 2012).
13. E. C. Bush, J. M. Allman, The scaling of frontal cortex in primates and carnivores. *Proc. Natl. Acad. Sci. U.S.A.* **101**, 3962–3966 (2004).
14. B. Jung *et al.*, A comprehensive macaque fMRI pipeline and hierarchical atlas. *Neuroimage* **235**, 117997 (2021).
15. A. E. Dorr, J. P. Lerch, S. Spring, N. Kabani, R. M. Henkelman, High resolution three-dimensional brain atlas using an average magnetic resonance image of 40 adult C57Bl/6J mice. *Neuroimage* **42**, 60–69 (2008).
16. N. Tzourio-Mazoyer *et al.*, Automated anatomical labeling of activations in SPM using a macroscopic anatomical parcellation of the MNI MRI single-subject brain. *Neuroimage* **15**, 273–289 (2002).
17. N. A. Nadkarni, S. Bougacha, C. Garin, M. Dhenain, J. L. Picq, A 3D population-based brain atlas of the mouse lemur primate with examples of applications in aging studies and comparative anatomy. *Neuroimage* **185**, 85–95 (2019).
18. R. Pijnenburg *et al.*, Myelo- and cytoarchitectonic microstructural and functional human cortical atlases reconstructed in common MRI space. *Neuroimage* **239**, 118274 (2021).
19. C. M. Garin *et al.*, Resting state functional atlas and cerebral networks in mouse lemur primates at 11.7 Tesla. *Neuroimage* **226**, 117589 (2021).
20. C. Liu *et al.*, A digital 3D atlas of the marmoset brain based on multi-modal MRI. *Neuroimage* **169**, 106–116 (2018).
21. Q. Wang *et al.*, The Allen mouse brain common coordinate framework: A 3D reference atlas. *Cell* **181**, 936–953.e20 (2020).
22. N. Vogt, A detailed marmoset brain atlas. *Nat. Methods* **17**, 251 (2020).
23. L. Fan *et al.*, The human brainnetome atlas: A new brain atlas based on connectional architecture. *Cereb. Cortex* **26**, 3508–3526 (2016).
24. P. J. Johnson *et al.*, Stereotactic cortical atlas of the domestic canine brain. *Sci. Rep.* **10**, 4781 (2020).
25. D. Stolzberg, C. Wong, B. E. Butler, S. G. Lomber, Catlas: An magnetic resonance imaging-based three-dimensional cortical atlas and tissue probability maps for the domestic cat (Felis catus). *J. Comp. Neurol.* **525**, 3190–3206 (2017).
26. S. E. John *et al.*, The ovine motor cortex: A review of functional mapping and cytoarchitecture. *Neurosci. Biobehav. Rev.* **80**, 306–315 (2017).
27. M. Laubach, L. M. Amarante, K. Swanson, S. R. White, What, if anything, is rodent prefrontal cortex? *eNeuro* **5**, ENEURO.0315-0318.2018 (2018).
28. D. Ongür, J. L. Price, The organization of networks within the orbital and medial prefrontal cortex of rats, monkeys and humans. *Cereb. Cortex* **10**, 206–219 (2000).
29. A. Dinopoulos, A. N. Karamanlidis, G. Papadopoulos, J. Antonopoulos, H. Michaloudi, Thalamic projections to motor, prefrontal, and somatosensory cortex in the sheep studied by means of the horseradish peroxidase retrograde transport method. *J. Comp. Neurol.* **241**, 63–81 (1985).
30. A. Kosmal, Subcortical connections of the prefrontal cortex in dogs: Afferents to the medial cortex. *Acta Neurobiol. Exp. (Warsz.)* **41**, 339–356 (1981).
31. A. Kosmal, Subcortical connections of the prefrontal cortex in dogs: Afferents to the proreal gyrus. *Acta Neurobiol. Exp. (Warsz.)* **41**, 69–85 (1981).
32. R. W. Cox, AFNI: Software for analysis and visualization of functional magnetic resonance neuroimages. *Comput. Biomed. Res.* **29**, 162–173 (1996).
33. D. Orme *et al.*, CAPER: Comparative analyses of phylogenetics and evolution in R. *Methods Ecol. Evol.* **3**, 145–151 (2013).
34. J. B. Smaers, F. J. Rohlf, Testing species' deviation from allometric predictions using the phylogenetic regression. *Evolution* **70**, 1145–1149 (2016).
35. M. R. E. Symonds, S. P. Blomberg, "A primer on phylogenetic generalised least squares" in *Modern Phylogenetic Comparative Methods and Their Application in Evolutionary Biology*, L. Garamszegi, Ed. (Springer, Berlin, Heidelberg, 2014), chap. 5, pp. 105–130.
36. M. F. Glasser *et al.*, A multi-modal parcellation of human cerebral cortex. *Nature* **536**, 171–178 (2016).
37. M. F. Glasser, D. C. Van Essen, Mapping human cortical areas in vivo based on myelin content as revealed by T1- and T2-weighted MRI. *J. Neurosci.* **31**, 11597–11616 (2011).
38. D. C. Van Essen, D. L. Dierker, Surface-based and probabilistic atlases of primate cerebral cortex. *Neuron* **56**, 209–225 (2007).
39. J. H. Kaas, The evolution of the complex sensory and motor systems of the human brain. *Brain Res. Bull.* **75**, 384–390 (2008).
40. G. Mendoza, H. Merchant, Motor system evolution and the emergence of high cognitive functions. *Prog. Neurobiol.* **122**, 73–93 (2014).
41. C. M. Garin *et al.*, An evolutionary gap in primate default mode network organization. *SSRN Elect. J.* 10.2139/ssrn.3806073 (2021).
42. J. R. Burger, M. A. George, C. Leadbetter, F. Shaikh, The allometry of brain size in mammals. *J. Mammal.* **100**, 276–283 (2019).
43. M. Gabi *et al.*, No relative expansion of the number of prefrontal neurons in primate and human evolution. *Proc. Natl. Acad. Sci. U.S.A.* **113**, 9617–9622 (2016).
44. J. B. Smaers *et al.*, Primate prefrontal cortex evolution: Human brains are the extreme of a lateralized ape trend. *Brain Behav. Evol.* **77**, 67–78 (2011).
45. S. Herculano-Houzel, P. R. Manger, J. H. Kaas, Brain scaling in mammalian evolution as a consequence of concerted and mosaic changes in numbers of neurons and average neuronal cell size. *Front. Neuroanat.* **8**, 77 (2014).
46. K. Zilles, Brodmann: A pioneer of human brain mapping-his impact on concepts of cortical organization. *Brain* **141**, 3262–3278 (2018).
47. K. Brodmann, Vergleichende Lokalisationslehre der Grosshirnrinde in ihren Prinzipien dargestellt auf Grund des Zellenbaues. (1909).
48. C. G. Schrago, C. A. Russo, Timing the origin of New World monkeys. *Mol. Biol. Evol.* **20**, 1620–1625 (2003).
49. P. Majka *et al.*, Open access resource for cellular-resolution analyses of corticocortical connectivity in the marmoset monkey. *Nat. Commun.* **11**, 1133 (2020).
50. B. B. Avants *et al.*, The Insight ToolKit image registration framework. *Front. Neuroinform.* **8**, 44 (2014).
51. P. A. Yushkevich *et al.*, User-guided 3D active contour segmentation of anatomical structures: Significantly improved efficiency and reliability. *Neuroimage* **31**, 1116–1128 (2006).